

BLOW-UP OF THE NONEQUIVARIANT (2 + 1)-DIMENSIONAL WAVE MAP

JÖRG FRAUENDIENER ¹ and RALF PETER¹

(Received 7 July, 2013; revised 24 September, 2013)

Abstract

It has been known for a long time that the equivariant 2 + 1 wave map into the 2-sphere blows up if the initial data are chosen appropriately. Here, we present numerical evidence for the stability of the blow-up phenomenon under explicit violations of equivariance.

2010 *Mathematics subject classification*: primary 35L53; secondary 35L70, 65M20, 65P10.

Keywords and phrases: wave map, blow-up, equivariance, symplectic integrator.

1. Introduction

The work presented here is a continuation of the investigation of the wave map system carried out by the same authors. Previously [7, 8] we presented our results on the blow-up in the equivariant case which we obtained by evolution of a 2 + 1 code that did not enforce the equivariance. As we pointed out, this is already an indication that the blow-up phenomenon is stable against perturbations of the size of the truncation error of the evolution algorithm used. In the present paper we give numerical evidence that this is also true for situations where initial data are used for which equivariance is broken explicitly at the level of the initial data.

For this investigation we have used the same set-up as previously [7], so we give only a brief description and refer the reader to that paper for the details.

1.1. The wave map system We use an extrinsic formulation of the 2 + 1 wave map, so we study maps U from (2 + 1)-dimensional Minkowski space \mathbb{M}^{2+1} into the unit sphere embedded into the Euclidean space \mathbb{R}^3 ,

$$U : \mathbb{M}^{2+1} \longrightarrow \mathbb{S}^2 \hookrightarrow \mathbb{R}^3, \quad (x^0, x^1, x^2) \longmapsto (z^1, z^2, z^3).$$

The unit sphere is described as usual as the zero set of the polynomial $\phi(z) = (z^1)^2 + (z^2)^2 + (z^3)^2 - 1 = \delta_{AB} z^A z^B - 1$, where we denote the Euclidean metric on \mathbb{R}^3 by δ_{AB} .

¹Department of Mathematics and Statistics, University of Otago, PO Box 56, Dunedin 9054, New Zealand; e-mail: joergf@maths.otago.ac.nz, rpeter@maths.otago.ac.nz.

© Australian Mathematical Society 2014, Serial-fee code 1446-1811/2014 \$16.00

This implies the restriction

$$\phi(U) = U^A U_A - 1 = 0 \quad (1.1)$$

on the map U .

The wave map equations are obtained from an action principle using the action

$$\mathcal{A}[U, \partial U] = \int_{\mathbb{M}^{2+1}} (\partial^a U^A \partial_a U_A + \lambda \phi(U)) dt dx dy. \quad (1.2)$$

Here (t, x, y) are Cartesian coordinates on \mathbb{M}^{2+1} and λ is a Lagrange multiplier used to implement the constraint (1.1).

Extremizing (1.2) with respect to U^A and λ leads to the Euler–Lagrange equations

$$\square_g U^A - \lambda U^A = 0, \quad U^A U_A - 1 = 0,$$

where \square is the usual d'Alembert operator $\square = \partial_{tt} - \partial_{xx} - \partial_{yy}$. It is possible to eliminate the Lagrange multiplier with the help of the constraint equation. However, we choose not to do this because in our numerical algorithm we solve the constraint and determine the Lagrange multiplier at every time step.

For the sake of clarity, we relabel the component functions of U as follows: $u := U^1$, $v := U^2$ and $w := U^3$. Then we can write the wave map system in the form

$$\begin{cases} \ddot{u} - \partial_{xx} u - \partial_{yy} u - \lambda u = 0, \\ \ddot{v} - \partial_{xx} v - \partial_{yy} v - \lambda v = 0, \\ \ddot{w} - \partial_{xx} w - \partial_{yy} w - \lambda w = 0, \end{cases} \quad (1.3)$$

$$\phi(u, v, w) = u^2 + v^2 + w^2 - 1 = 0. \quad (1.4)$$

This system has two nontrivial static solutions U_S ,

$$u_S(x, y) = \frac{2x}{1 + x^2 + y^2}, \quad v_S(x, y) = \frac{2y}{1 + x^2 + y^2}, \quad w_S(x, y) = \pm \frac{1 - x^2 - y^2}{1 + x^2 + y^2}. \quad (1.5)$$

They describe the inverse of the stereographic projection to the sphere from the north (respectively, south) pole.

1.2. Blow-up dynamics The key feature to investigate the blow-up of the $(2 + 1)$ -dimensional wave map system is the scaling invariance of the equations (holds in all dimensions) and the energy (only in $2 + 1$ dimensions). This means that the equations as well as the energy are invariant under the transformation

$$(t, x, y) \longrightarrow (st, sx, sy) \quad \text{with } s \in \mathbb{R}.$$

Due to the fact that the energy is also scaling invariant, the $(2 + 1)$ -dimensional case is called the energy critical case.

The first numerical results on the blow-up of the equivariant system were obtained by Bizoń et al. [4]. The following three observations were made:

- (i) When the energy of the initial data is too large, a singularity will form. Later, Sterbenz and Tataru [10] specified in more detail under what conditions the 2 + 1 wave map with the 2-sphere as target has nonsingular solutions.
- (ii) Close to the blow-up it is possible to rescale the dynamical solution U of (1.3) so that it approximates (in an appropriate Sobolev space) the static solution (1.5):

$$\lim_{t \nearrow T} U(t, s(t)x, s(t)y) = U_S(x, y),$$

where T is the blow-up time and $s(t)$ is the so-called scaling function. The blow-up (or the singularity formation) appears as a shrinking of the rescaled static solution (1.5). This result was proven by Struwe [11]. In the same article it was also shown that the existence of a nontrivial static solution is necessary for singularity formation. The scaling function $s(t)$ can be used to detect how the singularity formation proceeds. This was used by Bizoń et al. [4] and the present authors [7] for the numerical investigation of the blow-up. Bizoń et al. [4] stated two properties for the scaling function: $s(t) > 0$ for $t < T$ (there is now no solution for $t > T$) and $s(t) \searrow 0$ for $t \nearrow T$. Raphaël and Rodnianski [9] as well as Ovchinnikov and Sigal [6] presented detailed work on the blow-up dynamics. In both articles, an analytical form for the scaling function $s(t)$ was obtained. Ovchinnikov and Sigal were able to reduce the number of free parameters and therefore give a more precise description of the scaling function $s(t)$.

- (iii) Towards the blow-up, the local kinetic energy at the point of the singularity formation goes to zero and the local potential energy approaches the value 4π , which is the energy of the static solution (1.5).

Those results were confirmed by Isenberg and Liebling [5]. In our previous work [7] we also observed the expected blow-up behaviour. In addition, we showed that the blow-up is stable under perturbations with a magnitude of the truncation error of the numerical scheme.

1.3. Numerical set-up The numerical method that we use to solve (1.3)–(1.4) is the same as in our previous paper [7]. Therefore, we only briefly outline the most important points here. We discretize the spatial derivatives in the action functional using fourth-order centred finite differences. This yields a semi-discrete action for finitely many degrees of freedom. The Euler–Lagrange equations for this action give Hamiltonian equations of motion which are symplectic by construction, that is, they preserve the canonical symplectic form of classical mechanics. The constraint (1.4) results in as many holonomic constraints as there are points on the numerical grid. In this way we obtain a Hamiltonian system with holonomic constraints. Our time integration method takes advantage of these properties: we use the Rattle method [1], a symplectic integrator for Hamiltonian systems with holonomic constraints.

As described in our previous paper [7], we use the unit square $\Omega = [0, 1] \times [0, 1]$ as our domain of integration with homogeneous Neumann boundary conditions at the outer boundary, that is, on the sides with $x = 1$ and $y = 1$, respectively. The other sides

we regard as lines of symmetry, thus effectively enlarging the domain of computation to the square $[-1, 1] \times [-1, 1]$. We use equal resolutions in both directions, that is, $\Delta x = \Delta y = 1/N$ on a grid with $N + 1$ grid points in each direction.

A different numerical approach to the wave map problem was presented by Bartels et al. [2, 3] who used a finite element approach for the spatial discretization. The three components of the solutions are visualized as a vector field. In this representation the blow-up is seen as a sharp change of the direction of the vectors near the origin. To follow the blow-up dynamics the authors track a semi-norm which reaches a maximum at the blow-up.

1.4. Initial data To guarantee that the constraint (1.4) is satisfied, the initial data are chosen as

$$\begin{aligned} u_0(0, x, y) &= \sin(\vartheta_0(r, \sigma)) \cos(\varphi_0(\sigma)), \\ v_0(0, x, y) &= \sin(\vartheta_0(r, \sigma)) \sin(\varphi_0(\sigma)), \\ w_0(0, x, y) &= \cos(\vartheta_0(r, \sigma)), \end{aligned}$$

where r and σ are polar coordinates in \mathbb{R}^2 related to the Cartesian coordinates x and y in the usual way:

$$x = r \cos(\sigma), \quad y = r \sin(\sigma).$$

Equivariance means that rotations in the (x, y) -plane in \mathbb{M}^{2+1} are mapped to rotations around the z -axis in \mathbb{R}^3 , and is reflected in this parametrization of the initial data as the requirement that

$$\vartheta_0(r, \sigma) = \vartheta_0(r), \quad \varphi_0(\sigma) = k\sigma \text{ with } k \in \mathbb{Z}.$$

In our choice of initial data we explicitly break the equivariance by making ϑ_0 depend on σ but we keep the reflection symmetry across the lines $x = 0$ and $y = 0$ discussed above. The function $\vartheta_0(r, \sigma)$ is defined as follows:

$$\begin{aligned} \vartheta_0(r, \sigma) &= \begin{cases} Ag(r)h(\sigma) & \text{for } r \in [r_1, r_2] \\ 0 & \text{otherwise,} \end{cases} \\ g(r) &= \left[4 \frac{r - r_1}{r_2 - r_1} \frac{r_2 - r}{r_2 - r_1} \right]^4, \\ h(\sigma) &= \begin{cases} h_0(\sigma) & \text{for } \sigma \in [0, \sigma_0] \\ 1 & \text{for } \sigma \in [\sigma_0, \pi/2 - \sigma_0] \\ h_0(\pi/2 - \sigma) & \text{for } \sigma \in [\pi/2 - \sigma_0, \pi/2], \end{cases} \end{aligned}$$

where $h_0(\sigma)$ is a monotonically increasing function with $h_0(0) = B$ and $h_0(\sigma_0) = 1$. It is chosen in such a way that h is at least C^4 ; see Figure 1. The function $h(\sigma)$ describes the deviation from equivariance, which corresponds to $h(\sigma) = 1$. The parameter B measures the strength of the deviation ($B = 1$ corresponds to the equivariant case). We choose $\varphi_0(\sigma) = \sigma$ as in the equivariant case with homotopy index $k = 1$.

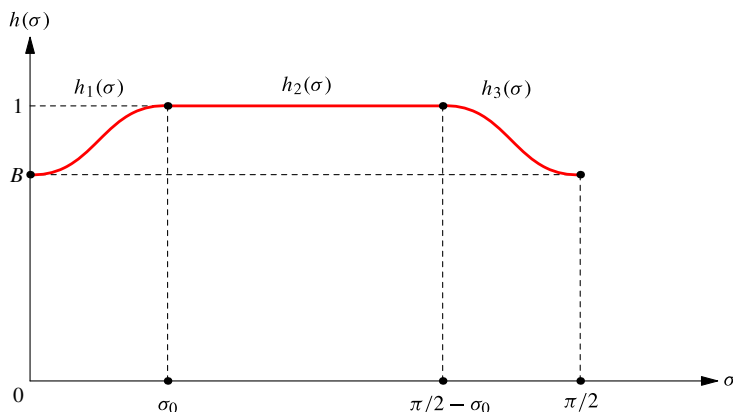


FIGURE 1. The angular perturbation function $h(\sigma)$.

The initial data for the velocities are chosen as

$$\begin{aligned} \dot{u}(0, x, y) &= \partial_r u = \cos \vartheta_0(r, \sigma) \vartheta'_0(r, \sigma) \frac{x}{r}, \\ \dot{v}(0, x, y) &= \partial_r v = \cos \vartheta_0(r, \sigma) \vartheta'_0(r, \sigma) \frac{y}{r}, \\ \dot{w}(0, x, y) &= \partial_r w = -\sin \vartheta_0(r, \sigma) \vartheta'_0(r, \sigma), \end{aligned}$$

where $\vartheta'_0(r)$ denotes the derivative of $\vartheta_0(r)$ with respect to its argument. These initial data describe a ring-shaped bump in the (x, y) -plane around the origin. The choice of the velocity initial data results in a shrinking of this ring towards the origin. After the function $w(t, x, y)$ reaches its minimum close to the origin, the wave packet expands again.

2. The scaling function

As described above, the blow-up dynamics are captured by the scaling function $s(t)$ between the solution and the approximated static solution. Previously [7] we described how we determine this function in the equivariant case: since w is an axisymmetric function $w(t, r)$, in that case we determine its second derivative with respect to r at $r = 0$ at every time t and find $s(t)$ as the appropriate factor between this and the second radial derivative of the static solution.

When equivariance is broken, w is no longer axisymmetric and we need to extract the scaling function from the full matrix of second derivatives, the Hessian, of w at the origin. The Hessian $H_S(t, x, y)$ of the rescaled static solution

$$w_S^s(t, x, y) := w_S(r(x, y)/s(t)) = \frac{1 - (r(x, y)/s(t))^2}{1 + (r(x, y)/s(t))^2}$$

at the origin is proportional to the identity matrix:

$$H_S(t, 0, 0) = -\frac{4}{s^2(t)} \mathbb{1}_2.$$

If the blow-up dynamics in the nonequivariant case are similar to the equivariant case, then close to blow-up the off-diagonal terms of the Hessian of the solution will be small compared to the diagonal terms and we can extract the scaling function $s(t)$ simply from the trace of the Hessian using

$$\text{tr } H_S(t, 0, 0) = -\frac{8}{s^2(t)}.$$

Alternatively, we could find $s(t)$ also by taking the determinant of the Hessian using

$$\det H_S(t, 0, 0) = \frac{16}{s^4(t)}.$$

Geometrically this just means that we take either the mean curvature or the Gauss curvature at the origin of the surface defined by the graph of w as the indicator for the scaling function. It turned out that there are no essential differences so we used the Gauss curvature throughout.

3. Blow-up results

In Section 1.2 the dynamics of the wave packet were described. We now give more details about the behaviour of the solution for initial data with large energy. If the energy of the initial data is large enough, one expects a singularity formation as presented by Bizoń et al. [4] and the present authors [7]. In our set-up, we interpret a change in the behaviour of $w(t, x, y)$ at the origin as the appearance of the blow-up. We have specified the initial data so that there remains a residual symmetry, namely the reflection symmetry with respect to both coordinate axes. This symmetry has the consequence that the value of the function w should remain constant, that is, with our initial data $w(t, 0, 0) = 1$ throughout the evolution. However, if the energy is too large the numerical solution suddenly jumps to $w(t, 0, 0) = -1$. From a geometrical point of view the solution switches from the stereographic projection from the south pole to the projection from the north pole, that is, it suddenly approximates *the other static solution*. This seems to be due to the numerical method we are using. The Rattle method for the time integration always forces the solution onto the constraint manifold. For large energies it becomes increasingly difficult for the iterative projection algorithm to find a solution. It seems that it is somewhat easier for the system to flip to the other solution.

Using the previously introduced methods, we are now able to analyse the blow-up dynamics and singularity formation in the nonequivariant case. This is analogous to the equivariant procedure presented previously [7]. For these simulations, the value of the deviation from the equivariance B is fixed and the amplitude A is increased towards

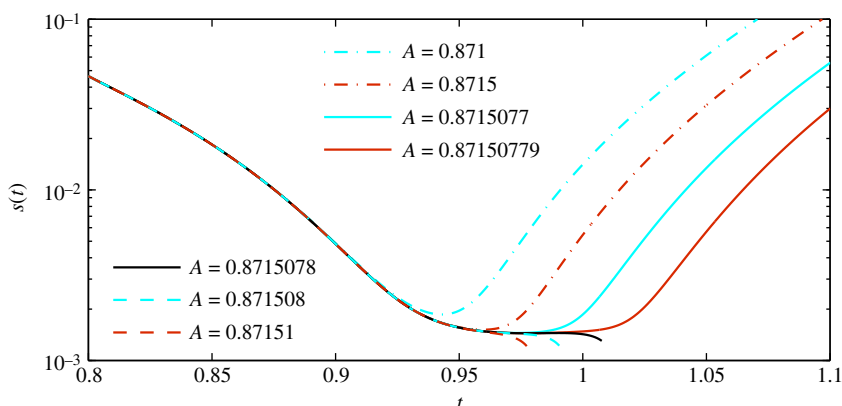


FIGURE 2. The scaling function $s(t)$ for different parameter values A and $B = 0.8$. The value $A^* = 0.871\,507\,80$ is the critical amplitude. Computed with $N = 1280$.

the critical value. As the indicator for the presence of the blow-up singularity we take the above mentioned flip from one static solution to the other.

The first step in the analysis of the blow-up is the determination of the critical amplitude A^* . Figure 2 shows the scaling function for different values of the amplitude A , where the parameter B is fixed to $B = 0.8$ and the numerical resolution is $N = 1280$. The qualitative behaviour is the same as in the equivariant case. An increase of the amplitude towards the critical value $A^* \approx 0.871\,507\,80$ leads to an increase in the time that the system remains in the quasi-static state. The appearance of this quasi-static, hovering state is due to the limited spatial resolution. If the number of grid points for the simulations is increased, the critical behaviour moves to higher values of the amplitude and reduces the duration of the hovering state. Therefore, our calculations are limited by the spatial resolution.

The next step is to determine the blow-up time T . This can be found by fitting the last sub-critical scaling function to the analytical expression [6]

$$s(t) = \frac{1.04}{e}(T - t) \exp(-\sqrt{-\ln(T - t) + b}). \quad (3.1)$$

This formula was derived for the equivariant case but if the blow-up dynamics are a stable phenomenon then close to blow-up this formula should apply to the nonequivariant case as well. We fit the curve for $A = 0.871\,507\,79$ to the function $s(t)$ defined in (3.1). This results in $T = 0.934\,851\,35$ for the blow up time and $b = -2.143\,534\,6$ for the parameter which depends on the initial data. The residual error for this fit was $8.032\,783\,8 \cdot 10^{-9}$. Figure 3 shows the result of the fitting procedure. The fit interval $t \in [0.865, 0.8816]$ was chosen as a compromise between being close enough to the blow-up time (lower time bound) and the time domain, where the scaling function numerically converges (upper time bound).

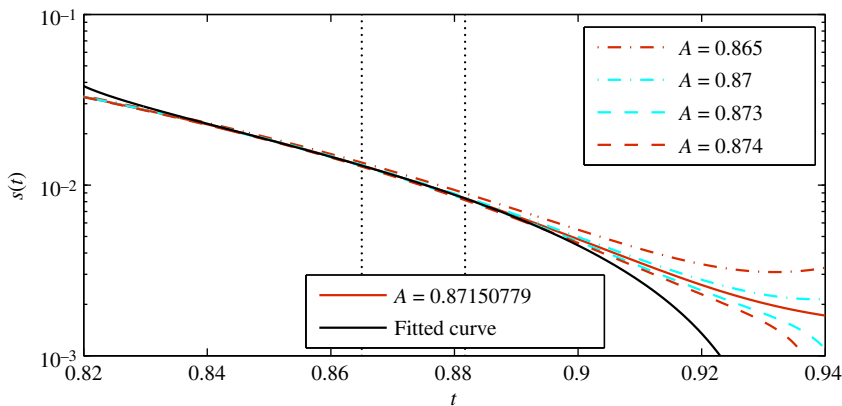


FIGURE 3. Fit of the scaling function $s(t)$ to the analytical expression, given by Ovchinnikov and Sigal [6]. The computed blow-up time is $T = 0.940\,945\,24$. The value $A = 0.871\,507\,79$ is the last sub-critical value shown, that is, for which the solution does not change its behaviour at the origin. Computed with $N = 1280$.

TABLE 1. Comparison of the ingoing wave packet along the x -axis and the diagonal.

	x -axis	Diagonal	Relative deviation
t_{\min}	0.929 687 5	0.929 375	$3.362\,474\,8 \cdot 10^{-4}$
$w_{\min}(t_{\min})$	-0.948 622 86	-0.948 678 28	$5.841\,811\,8 \cdot 10^{-5}$
$w_{\min}(0)$	0.766 638 99	0.643 675 01	0.191 034 26

We now describe how the rescaled dynamical solution approximates the equivariant harmonic map near the blow-up. Since equivariance is broken, this process is no longer isotropic but instead depends on the angle σ . Figure 4 shows the graphs of the component $w(t, x, y)$ taken along the x -axis and along the diagonal. As time progresses, the profiles are in better and better agreement. This being the case, Figure 5 shows the successive stages of the rescaled dynamical solution taken only along the x -axis.

To measure the deviation from the equivariant case, the difference between the two time steps when each of the wave packets reach their minimum is used. Additionally, the difference in the minima itself is used. Table 1 shows the numerical results of the two rescaled wave packets. The time t_{\min} is defined as the time when the wave packet along the x -axis, or the diagonal line $y = x$, reaches its minimum $w_{\min}(t_{\min})$. Based on these results, the relative deviation between the respective values is computed. Additionally, the respective minima $w_{\min}(0)$ at $t = 0$ are shown.

From the results in Table 1 and the graphs we conclude that the difference between the profiles along the x -axis and $y = x$ vanishes during the evolution. The deviation along the two lines becomes significantly smaller, ending in nearly rotational symmetry.

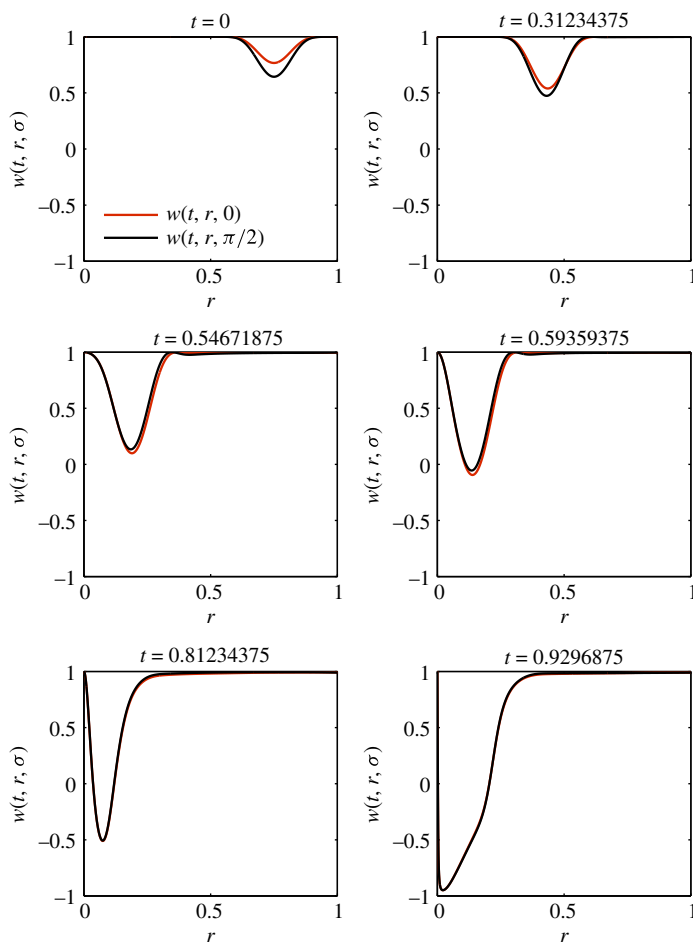


FIGURE 4. Time evolution of the wave packet for the amplitude $A = 0.871\ 507\ 79$. The slices along the x -axis and along the diagonal $y = x$ are shown.

4. Conclusions

We have presented here for the first time numerical indications for a blow-up and singularity formation in the nonequivariant (2 + 1)-dimensional wave map system. The methods which were developed for the analysis of the equivariant case of this system were extended and generalized to the nonequivariant case. It was possible to show that initial data, which are nearly equivariant, can also lead to blow-up behaviour similar to the equivariant case.

However, our simulations also showed the need for higher numerical resolutions in the two-dimensional nonequivariant case to get a deeper and more detailed view of the blow-up dynamics and singularity formation. This can be done with grid refinement

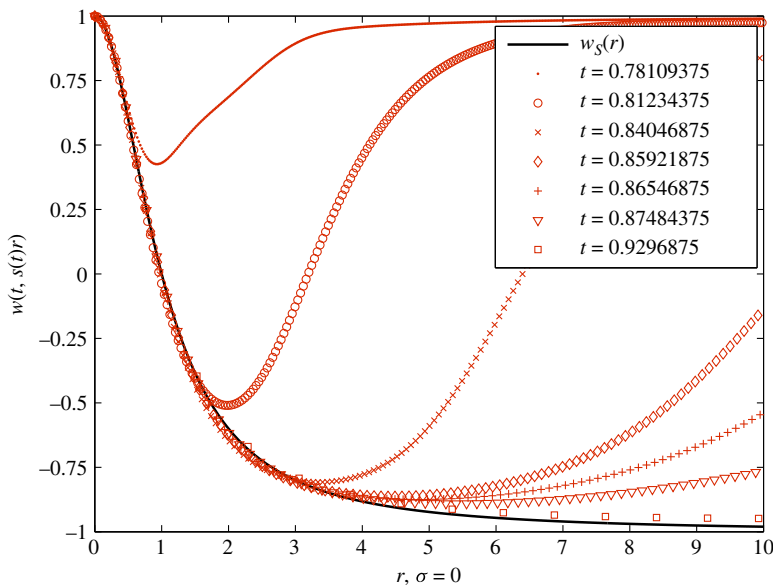


FIGURE 5. Ingoing wave packet for $A = 0.871\,507\,79$ and $B = 0.8$ rescaled with the scaling function $s(t)$ for various values of t along the x -axis. The rescaled functions $w(t, s(t)r)$ approximate the static solution $w_S(r)$. The function $w(t, r)$ reaches its minimum at $t = 0.929\,687\,5$.

techniques or by completely changing the spatial discretization of the equations. The use of (pseudo-)spectral methods may be appropriate in this respect.

Acknowledgements

Ralf Peter was supported by a DAAD and a University of Otago Doctoral Scholarship. This research was partially funded by the Royal Society of New Zealand via the Marsden Fund.

References

- [1] H. C. Andersen, “Rattle: a ‘velocity’ version of the SHAKE algorithm for molecular dynamics calculations”, *J. Comput. Phys.* **52** (1983) 24–34; doi:10.1016/0021-9991(83)90014-1.
- [2] S. Bartels, X. Feng and A. Prohl, “Finite element approximations of wave maps into spheres”, *SIAM J. Numer. Anal.* **46** (2007) 61–87; doi:10.1137/060659971.
- [3] S. Bartels, “Semi-implicit approximation of wave maps into smooth or convex surfaces”, *SIAM J. Numer. Anal.* **47** (2009) 3486–3506; doi:10.1137/080731475.
- [4] P. Bizoń, T. Chmaj and Z. Tabor, “Formation of singularities for equivariant $(2 + 1)$ -dimensional wave maps into the 2-sphere”, *Nonlinearity* **14** (2001) 1041–1053; doi:10.1088/0951-7715/14/5/308.
- [5] J. Isenberg and S. L. Liebling, “Singularity formation in $2 + 1$ wave maps”, *J. Math. Phys.* **43** (2002) 678–683; doi:10.1063/1.1418717.
- [6] Yu. N. Ovchinnikov and I. M. Sigal, “On collapse of wave maps”, *Phys. D* **240** (2011) 1311–1324; doi:10.1016/j.physd.2011.04.014.

- [7] R. Peter and J. Frauendiener, “Free versus constraint evolution of the $2 + 1$ equivariant wave map”, *J. Phys. A* **45** (2012) 055201; doi:10.1088/1751-8113/45/5/055201.
- [8] R. Peter, “Numerical studies of geometric partial differential equations with symplectic methods”, Ph. D. Thesis, University of Otago, 2012.
- [9] P. Raphaël and I. Rodnianski, “Stable blow up dynamics for the critical co-rotational wave maps and equivariant Yang–Mills problems”, *Publ. Math. Inst. Hautes Études Sci.* **115** (2012) 1–122; doi:10.1007/s10240-011-0037-z.
- [10] J. Sterbenz and D. Tataru, “Regularity of wave maps in dimension $2 + 1$ ”, *Comm. Math. Phys.* **298** (2010) 231–264; doi:10.1007/s00220-010-1062-3.
- [11] M. Struwe, “Equivariant wave maps in two space dimensions”, *Comm. Pure Appl. Math.* **56** (2003) 815–823; doi:10.1002/cpa.10074.